



Experimental and numerical assessment of energy absorption capacity of thin-walled Al 5083 tube produced by PTCAP process

A. HOSSEINI, D. RAHMATABADI, R. HASHEMI, H. AKBARI

School of Mechanical Engineering, Iran University of Science and Technology, Tehran, Iran

Received 3 May 2019; accepted 15 October 2019

Abstract: The energy absorption capacity of the Al5083 thin-walled tube produced by parallel tubular angular pressing (PTCAP) process was evaluated. Also, microstructure, mechanical properties, and anisotropy coefficients were studied in the peripheral and axial directions. Results showed that values of energy absorption decreased with processing pass increasing and the values for the unprocessed, first and second passes were obtained to be 167, 161.4 and 160.7 J, respectively. The differences between the simulation results for the energy absorption values and their experimental values for the unprocessed, the first and the second PTCAP passes samples are about 5%, 10%, and 13%, respectively. The energy absorption capacity was related to the anisotropy coefficient and microstructure. The results demonstrated that grain refinement occurred and ultimate tensile strength (UTS) and microhardness after the first and second PTCAP passes were enhanced, while the increase rate in the first pass was much severer. Also, by applying PTCAP, the deformation modes were altered, such that the deformation mode of the annealed tube was quite symmetrical and circular while for the first and second passes there have been triple and double lobes diamond. The results of the numerical simulation for the deformation mode of the annealed and PTCAPed tubes were consistent with the experimental results. The deformation mode of tubes is dependent on their mechanical properties and variation of the mechanical properties during PTCAP process.

Key words: energy absorption; Al 5083; ultra-fine grained aluminum alloy; thin-walled tube; severe plastic deformation; anisotropy coefficient

1 Introduction

Thin-walled tubes have been utilized because of their characteristics such as lightness, high absorption capacity, high energy-to-weight ratio, and high formability [1,2]. The tubes have the highest absorption and impact absorption capacity, in proportion to their unit length and mass units. So, this advantage is a logical reason for using tubes as energy absorbers [3]. For example, the local buckling of tubes under axial compressive loading was compared with the deformation caused by the peripheral compressive loading in the rigid plates, and it was found that the energy capacity in the axial compressive loading is about ten times greater

than that of the peripheral compressive loading [4]. In the study of static crushing structure, the elastic energy range is usually ignored because plastic energy is much larger than elastic energy. Therefore, in this kind of deformation mechanism, the mechanical behavior of circular columns is often studied by assuming a rigid-plastic material model [5]. In general, collapse involves plastic buckling and the formation of symmetric and asymmetric progressive folding [6]. GUPTA and VENKATESH [7] investigated the effects of the diameter and thickness of the wall in the cylindrical tubes considering their axial collapse. Their numerical analysis showed that the energy absorption curve and different folding states for tubes with varying ratios of diameters to

thicknesses had good agreement with experimental results. LI et al [8] investigated the influence of geometry on energy absorption for AZ31B and A6063Al thin-walled square tubes through applying axial compression test with varying lengths at different compression rates. The results show that material and geometry are very effective, and by an increase in the L/W ratio (L and W represent the tube length and width, respectively), the maximal force and global specific energy absorption decreased for the magnesium tubes, while they remained approximately constant for the aluminum tubes. LINUL et al [9] studied the effect of temperature on the mechanical behavior of closed-cell aluminum-alloy foam-filled tubes (FFTs) under quasi-static compressive loads. The results indicated that at each tested temperature, the closed-cell aluminum foam improves the mechanical properties of the empty steel tubes. Also, they observed that the deformation mechanism of FFTs at all tested temperatures is axisymmetric concertina mode with the formation of two folds. Also, LINUL et al [10] concluded that the addition of particles decreased volumetric energy absorption of ZA27 metallic syntactic foam at elevated temperatures. ABDUL-LATIF et al [11] improved energy absorption in the axial plastic collapse of hollow cylinders. They used rigid steels in a pipe environment at different distances, which forced the tube to collapse from these rigid rings around the pipe. Their laboratory studies were carried out on copper and aluminum pipes with different ratios of radius to length and radius to thickness. TASDEMIRCI [12] examined the influence of tube end constraining on the axial crushing behavior of an aluminum tube. His results showed that in addition to the specifications of tube dimensions and material, the constraining of the two ends of the tube also affected the characteristics of axial crushing behavior and energy absorption.

In recent decades, there have been many attempts to improve the mechanical properties of materials [13]. One of the most successful ones is

severe plastic deformation (SPD). In all of SPD methods the principles are the same, without changing the geometric dimensions of the material during different SPD methods, it is possible to apply a high shear plastic strain and achieve the desired mechanical properties and the production of ultrafine-grained (UFG) and nanostructured (NS) materials [14]. Different SPD methods have been proposed, such as equal channel angular pressing (ECAP) [15–18], high-pressure torsion (HPT) [19–21] and accumulative roll bonding (ARB) [22–27] for bulk and sheet metal.

In contrast, suitable methods for producing tubes are high-pressure tube twisting (HPTT) [28], accumulative spin bonding (ASP) [29], tubular channel angular pressing (TCAP) [30] and parallel tubular angular pressing (PTCAP) [31]. PTCAP method as a novel SPD method was presented by FARAJI et al [31]. This process has several advantages over other methods such as reduction of process force and more uniformity of strain in the thickness of the tube.

In this research, the energy absorption capacity of the ultra-fine grained Al5083 tube produced by PTCAP process during different cycles has been presented. After PTCAP process, the mechanical properties and microstructure in each cycle have been evaluated experimentally. Besides, the axial buckling and absorption energy as the main goals have been investigated experimentally and numerically.

2 Experimental

2.1 Research material

In this work, Al5083 alloy was used as the raw material with the chemical composition and mechanical properties presented in Table 1. The tubes were prepared with the length, outer diameter, and thickness of 30, 20 and 2.5 mm, respectively. The prepared tubes were annealed at a temperature of 345 °C for 2 h to get a more homogeneous microstructure.

Table 1 Chemical composition and mechanical properties of Al5083 tube

Chemical composition/wt.%	Microhardness (HV)	Peripheral direction		Axial direction	
		UTS/MPa	Elongation/%	UTS/MPa	Elongation/%
Balance Al, 4–4.8 Mg, 0.6–1.0 Mn, 0.4 Fe, 0.4 Si, 0.3 Zn, 0.1 Cu, 0.1 Ti	74	465.8	26.4	231.6	18.4

2.2 PTCAP process

Figure 1 presents schematically the principle of the PTCAP process, which was used to produce the ultrafine-grained Al5083 tubes. According to Fig. 1, the PTCAP process includes two half passes. In the 1st half pass, at first, punch presses the tube into the gap between the mandrel and die consisting of two shear zones to increase the tube diameter to its maximum value. Then, the tube is pressed back using the second punch in the second half pass to decrease the tube diameter to its primary value. After N cycles of PTCAP process, the total equivalent plastic strain can be calculated through the following equation [31]:

$$\bar{\varepsilon}_{TN} = 2N \left\{ \sum_{i=1}^2 \left[2 \cot \left(\frac{\varphi_i}{2} + \frac{\psi_i}{2} \right) + \psi_i \operatorname{cosec} \left(\frac{\varphi_i}{2} + \frac{\psi_i}{2} \right) \right] / \sqrt{3} \right\} + \frac{2}{\sqrt{3}} \ln \frac{R_2}{R_1} \quad (1)$$

where φ , ψ , N , R_1 and R_2 are channel angle, curvature angle, number of cycles, primary and secondary radius, respectively.

Also, Fig. 1 illustrates PTCAP parameters and dimensions. MoS₂, as a lubricant, has been used to reduce the friction between the tubes and die [32,33]. The first, second, and third passes of PTCAP process were done to the tube at a ram speed of 5 mm/min at room temperature. The tube had no rotation toward the die between two-half cycles.

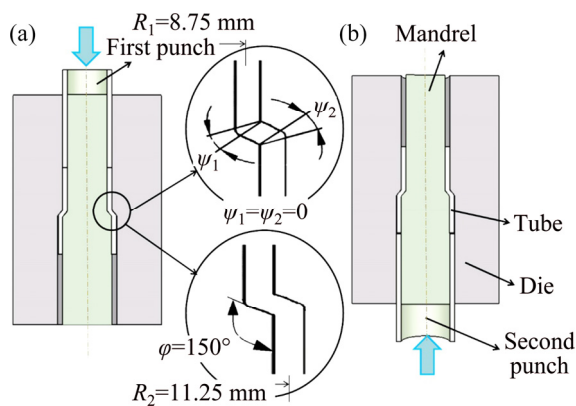


Fig. 1 Schematic illustration of PTCAP process and equipment: (a) The first half pass; (b) The second half pass [31]

2.3 Characterization tests

Microstructure and mechanical properties were investigated by optical microscopy, uniaxial tensile test and microhardness measurement for

unprocessed and processed materials after the first and second PTCAP passes. All of the mechanical properties have been reported in both axial and peripheral directions at room temperature.

The unprocessed and processed tubes after each PTCAP pass were cut by wire cut machining. Then, they were ground using 100–5000 sandpaper and polished by use of a mixture of alumina powder with a particle size of 0.5–0.1 μm , water, and soap. Finally, to remove the oxide layers, they were polished by alcohol and alumina without using water.

According to Figs. 2(a) and (b), the uniaxial tensile test samples were prepared for the primary and PTCAPed tubes in the axial and peripheral directions, respectively. The uniaxial tensile tests were performed at a nominal initial strain rate of $5 \times 10^{-4} \text{ s}^{-1}$ at room temperature using a SANTAM tensile testing machine. According to ASTM E08-10, the specimens were prepared with a gage length and a width of 10.6 and 1.8 mm in the axial direction and 10.6 and 3.5 mm in the peripheral direction, respectively. A fixture of the tensile test and fractured samples in both axial and peripheral directions is shown in Fig. 2.

Vickers microhardness tests were conducted using a JENUS apparatus under a load of 200 g

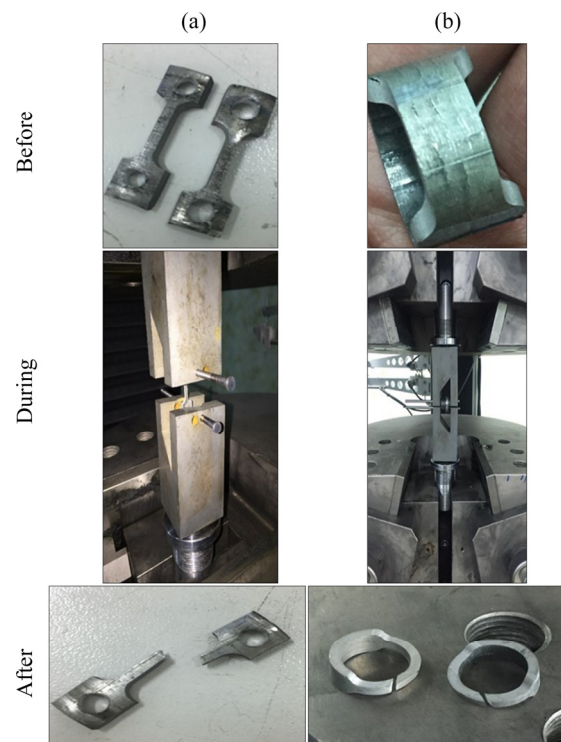


Fig. 2 Tensile test samples before, during and after examination: (a) Axial direction; (b) Peripheral direction

applied for 10 s. Microhardness tests were implemented at ten different points randomly in the axial and peripheral directions for the unprocessed and processed tubes. Then, for each sample, the minimum and maximum hardness values were disregarded.

2.4 Experimental and numerical buckling test

In this study, to determine the influence of PTCAP process on energy absorption, we prepared three samples from unprocessed Al5083, the first and second PTCAP passes. The wire-cut machine is used to prepare the samples to reduce the residual stress in the same dimensions (30 mm in length and 2.5 mm in thickness).

The fixture is made up of two upper and lower parts. The lower part is placed on the press machine table, and the upper part is placed under the press ram. The pressure is applied to the end of the upper part. A quasi-static axial buckling test is performed in identical fixing conditions using a SANTAM 50-ton press machine at a cross-head rate of 4 mm/min at room temperature. It is also possible to achieve the average of absorbed energy values, which is the area under the force–displacement curve. Deformation mode is visible from the folding tubes.

The finite element method is used to calculate the necessary deformation force, the amount of absorbed energy and the deformation modes in the study of the axial buckling behavior of the ultra-fine grained Al5083 tube processed by PTCAP process. For this purpose, the Abaqus/ Explicit 6.10 software is used. The model consists of tubes, up and down fixers so that the modeling conditions are precisely equal to the experimental conditions. Since all deformations are not symmetric, 3D modeling is done. The thin-walled tubes are considered as deformable components, and shell elements are used for their simulation. Fixators are modeled as rigid parts. The material properties of each cycle are extracted from the uniaxial tensile tests in both longitudinal and peripheral directions to consider anisotropic behavior of material according to Hill's 48 criteria. The Holloman's rule is used for predicting work-hardening, and the Holloman's equation is as follows:

$$\bar{\sigma}_y = k(\bar{\varepsilon})^n \quad (2)$$

where $\bar{\sigma}_y$, k , $\bar{\varepsilon}$ and n are the effective stress,

strength coefficient, effective plastic strain, and strain hardening exponent, respectively.

In this simulation, Dynamic/Explicit solving is used, and time is considered to be 0.3 s for complete deformation in the axial buckling test. In the load section, the bottom fixture is free, and the top fixation is given 10 mm of displacement. The effect of friction is considered using the penalty method, and a friction coefficient of 0.25 is applied. The shape, technique, algorithm, size, and the number of elements are supposed to be Quad-dominated, free, medial axis, 0.4 mm (size) and 9782 elements after checking mesh sensitivity. This element is considered the same for all samples. Due to the large deformation during the simulation, the convergence of the adaptive molding or automatic mating is used. Also, in the modeling, the following assumptions are considered.

- (1) The initial thickness of the tubes is uniform everywhere.
- (2) The two ends of the thin-walled tubes inside the fixture are quite constant.
- (3) Fixers are rigidly assembled and remain in constant shape.
- (4) The friction coefficient of all surfaces is the same.

3 Results

3.1 Microstructure and mechanical properties

Figure 3 shows the optical images of the unprocessed and PTCAP processed Al5083 thin-

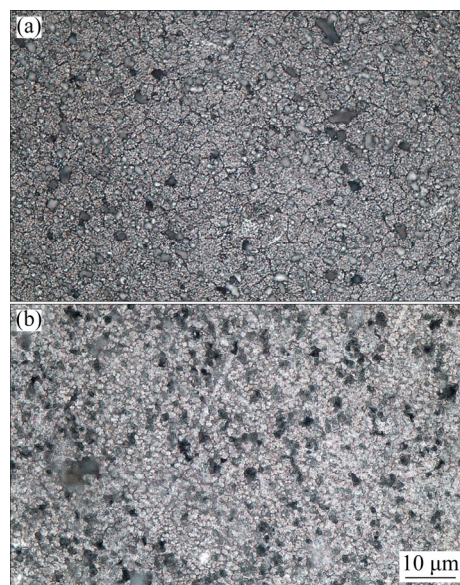


Fig. 3 Optical images of Al5083 tubes: (a) Unprocessed; (b) After the second PTCAP process

walled tubes at the second pass. In Fig. 3(a), a recrystallized homogeneous microstructure of the unprocessed Al5083 with a mean grain length of less than $10\ \mu\text{m}$ is observed. The microstructure of tube after the second PTCAP pass containing elongated ultrafine grains is demonstrated in Fig. 3(b). Also, from the comparison of the microstructure for both peripheral and axial directions, it can be seen that more grain refinement occurred in the peripheral direction.

Figures 4(a) and (b) show the engineering stress–strain curves in both the peripheral and axial directions at the room temperature, respectively. Also, variations of ultimate tensile strength and elongation in both the peripheral and axial directions which are extracted from engineering stress–strain, are demonstrated in Figs. 4(c) and (d). According to Fig. 4, as is evident at first glance, by applying severe plastic strain to the material, the strength increased, and the elongation reduced. After the first pass of PTCAP process, the UTS increased, and elongation decreased, drastically in

both the peripheral and axial directions. The UTS increased after the first cycle, in the peripheral and axial directions from 465.8 and 231.6 for unprocessed Al5083 to 547.7 and 310.4 MPa, respectively. However, the elongation in both directions decreased from 26.4 and 18.4 to 16.6 and 9.3 in the peripheral and axial directions, respectively. Major changes in mechanical properties are at the first cycle, and then variations of the mechanical properties are negligible. Though, after the first PTCAP pass, the strength increased at meager rates. The highest strength at the end of the second pass is obtained in both directions. This phenomenon has been demonstrated by similar studies in different UFG metals [31,34–38]. Finally, after the second PTCAP process, the values of UTS in peripheral and axial directions reach 579.4 and 337.5 MPa that are 1.24 and 1.46 times the unprocessed tube, respectively. In general, in all processes of severe plastic deformation, two mechanisms of strain hardening (increasing the density of dislocations) and grain refinement play

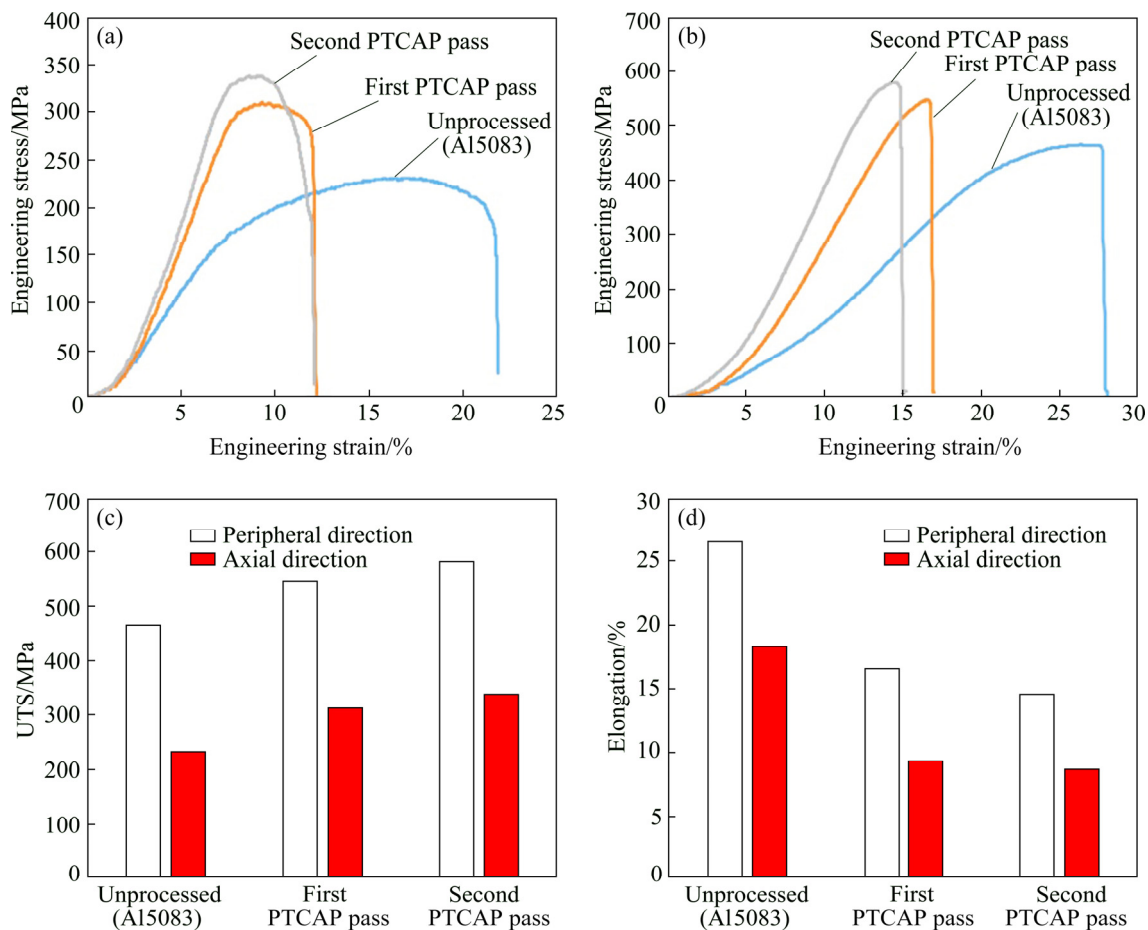


Fig. 4 Engineering stress–strain curves in axial direction (a) and peripheral direction (b), and variation of UTS (c) and elongation (d)

major roles in improving mechanical properties [39–41]. Also, according to the famous Hall–Petch equation, the grain size of microstructure plays an essential role in the mechanical properties of the metals, and by changing the coarse grain into the fine and ultra-fine grain, the mechanical properties increased [14,39,42]. As shown and expected, better mechanical properties (strength and formability) are achieved in the peripheral direction in comparison to the axial direction. Mechanical properties are improved at a higher rate in the peripheral direction compared to the axial direction, which is consistent with results of similar research, and can be caused by variation of crystallographic texture during the PTCAP process [32,34,43].

Figure 5 presents the microhardness measurements in both the peripheral and axial directions for annealed thin-walled tubes and after the first, second and third PTCAP passes. It is clear that, after the first pass of PTCAP processing, the values of Vickers microhardness increase, and for the second and third passes, the values are enhanced with low range compared to the first pass. Such as strength and formability, the high microhardness is achieved in the peripheral direction compared to the axial direction that can be attributed to the variation of crystallographic texture during the PTCAP process [32,34,43,44]. Also, the variation of Vickers microhardness is related to both the dominant mechanism in the PTCAP process: grain refinement and work hardening [14,37–39,45,46]. Finally, the maximum values of microhardness in the peripheral

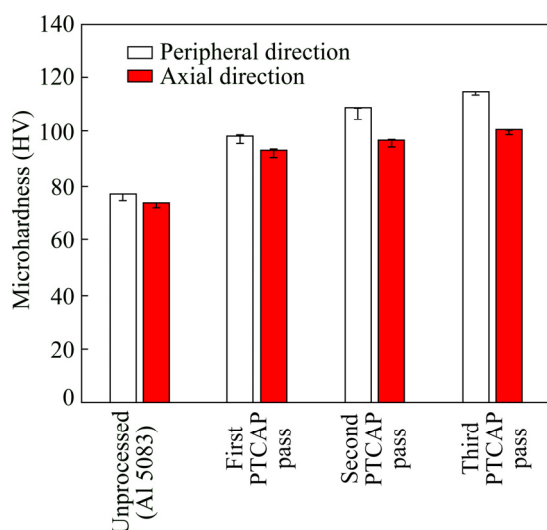


Fig. 5 Variation of microhardness in peripheral and axial directions after different PTCAP passes

and axial directions are obtained at the third PTCAP pass, and the microhardness values reach HV 114.9 and HV 100.7 that represent an improvement of 49% and 34% relative to the unprocessed Al5083 tubes, respectively.

3.2 Axial crushing test

Generally, the analysis of force–displacement diagrams in the quasi-static loading of tubes shows that the axial load increases to the first of folding formation (Maximum force) and then depending on the geometric parameters (such as diameter to thickness and length to diameter ratios), as well as material properties, occurring of different modes are possible. In general, its collapse involves plastic buckling and the formation of asymmetric and asymmetric progressive folding. The formation of the folding causes the force curve to go up and down. As it is known, the absorption rate of the thin-walled tubes depends mainly on their collapse behavior, thus, if the method of its collapse cannot be predicted accurately, determination of the exact absorption of energy will be impossible. Also, the tube length during the collapse is always a percentage of their initial length, and it is not promising to consider the length of the collapse equal to the length of the tube.

Images of the annealed and PTCAP processed thin-walled tubes during the axial buckling test are shown in Fig. 6. The applying PTCAP process alters the deformation modes of thin-walled tubes. Moreover, the deformation modes obtained from numerical simulations are entirely consistent with experimental results. According to Fig. 6, the deformation mode of the annealed tube is quite symmetrical and circular while deformation modes for the first and second PTCAPed samples are triple and double lobes diamond, respectively. The deformation modes of these thin-walled tubes are dependent on their mechanical properties obtained from the tensile test. However, as low-strength and high-strength tubes are more exposed to symmetrical circular and diamonds modes of deformation, respectively [6]. The most important and most effective parameter on the folding mode is anisotropy. By comparing the processed and unprocessed tubes, in addition to mechanical properties, the microstructure also varies, but due to the more significant anisotropy effect, the results are in good agreement with each other. Of course,

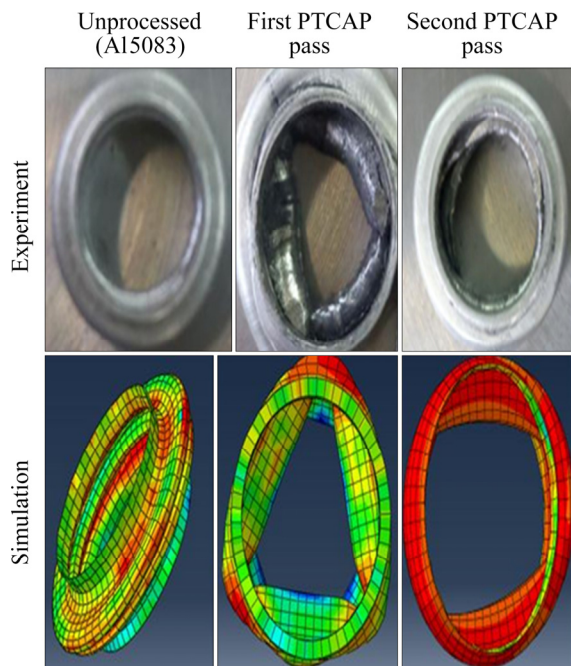


Fig. 6 Deformed unprocessed and PTCAP processed thin-walled tubes after axial crushing test experimentally and numerically

the microstructure is quite effective in mechanical properties and anisotropy, and its effects on the deformation mode are also considered in simulation indirectly. The force–displacement diagrams obtained from the quasi-static buckling test are shown in Fig. 7. As can be seen, the maximum force of folding is related to the yield force of tubes, and by applying the PTCAP process, the yield strength, and consequently, the maximum buckling force increase. After the maximum force (linear force–displacement relation), the axial buckling begins and the first folding forms, and after the formation of folding, the force decreases. This process is repeated to create each folding so that the tube is completely folded. This trend is shown in Fig. 7 for all three samples. Also, the amount of absorbed energy is obtained using the Q-mat software to calculate the surface under the force–displacement curve (Fig. 7). The computed absorbed energy values for the unprocessed, the first and the second PTCAP passes samples are 167, 161.4, and 160.7 J, respectively (Table 2). As it is known, the energy absorption values by the application of the PTCAP process decrease, and they decrease by about 3.35% and 3.77% in the first and second passes, respectively. Reducing energy can be due to reasons such as applying high strain,

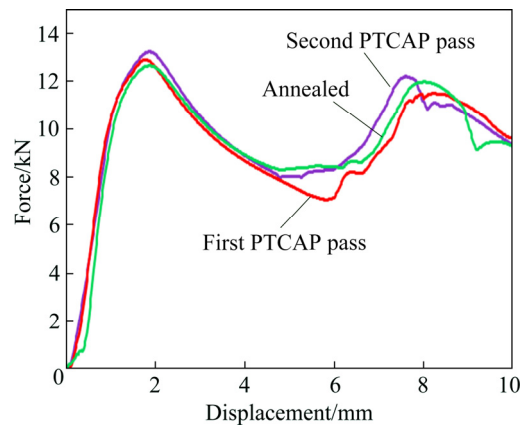


Fig. 7 Force–displacement curves for initial and PTCAP processed thin-walled tubes after axial crushing test

creating micro surface cracks, reducing the ductility, and reducing the anisotropy coefficient during the PTCAP process. AFRASIABI et al [47] investigated the influence of anisotropy on energy absorption in thin-walled tubes. They reported that by increasing the anisotropy coefficient ($R = (\text{peripheral ultimate tensile strength}) / (\text{axial ultimate tensile strength})$), the amount of energy absorbed by thin-walled tubes increased. The criterion of mechanical anisotropy has been defined as the ultimate peripheral strength to ultimate strength ratio. According to the results of the tensile test in the peripheral and axial directions, the defined anisotropy values for the primary Al5083 tube and after the first and second passes of PTCAP process are calculated as 2.01, 1.76 and 1.72, respectively. These results indicate that the amounts of anisotropy for Al5083 during the first and second passes of PTCAP decrease by 12.4% and 14.4% compared to the annealed thin-walled tubes, respectively. It can be seen that after the second pass despite the application of the high strain, it remains constant approximately.

In this study, the anisotropy coefficient decreases after the first and second PTCAP passes, continuously, and the trend of the anisotropy coefficient variations and absorbed energy changes are the same, approximately. Also, AFRASIABI et al [48] reported that applying severe plastic deformation to Cu–Zn thin-walled tube leads to the formation of UFG and NS, and this structure exhibits higher energy absorption capacity compared to coarse-grained materials. AFRASIABI et al [47] also reported that the anisotropy coefficient of the Cu–Zn thin-walled tube increased

Table 2 Summary of mechanical properties of samples obtained in this study

Sample	Peripheral direction			Axial direction			Anisotropy coefficient, R	Absorption energy/J
	UTS/MPa	Elongation/%	Microhardness (HV)	UTS/MPa	Elongation/%	Microhardness (HV)		
Annealed	465.8	26.4	77.1	231.6	18.4	74	2.01	167
First pass	547.7	16.6	98.6	310.4	9.3	93.4	1.76	161.4
Second pass	579.4	14.5	109	337.5	8.6	96.8	1.72	160.7

after applying severe plastic deformation to the material. They stated that the dominant deformation mechanism in Cu–30%Zn alloy was twinning for its low stacking fault energy (SFE). They showed that Cu–30%Zn alloy deformed by both slip and twinning mechanisms. In low stacking fault energy materials, the twinning mechanism is preferred to be slip mechanism because of the lower activation energy of twinning. Free slip line distance reduces due to the presence of twins. Twins–matrix interface operates as an obstacle to strain accommodation, and dislocation mobility is more complicated because of the reduction of the mean slip length. In the present study, the anisotropy coefficient of the PTCAP processed tube decreased. This result might be discussed by referring to the high stacking fault energy of Al5083 [25].

However, applying high strain to metal, to reduce grain size can decrease formability, and increase brittleness. So, it can lead to lower energy absorption capacity [49–51]. Generally, toughness and absorbed energy depend on both strength and formability. So, to achieve high energy absorption, both parameters need to be simultaneously increased, or the increase rate in one should be more severe than the decreased rate on another parameter [45,46,49]. Figure 8 shows the force–displacement diagrams obtained from the buckling test experimentally and numerically for the annealed, and the first and the second PTCAP passes samples. As can be seen, there is good agreement between empirical and numerical results. Also, the trends of variation of force in the linear elastic region and the formation of first folding coincide. The differences between the simulation results for the energy absorption values and their experimental values for the unprocessed, the first and the second PTCAP passes samples are about 5%, 10%, and 13%, respectively. The main reason for the error in the first and second PTCAP process can be due to the inability of the software to consider microstructure changes.

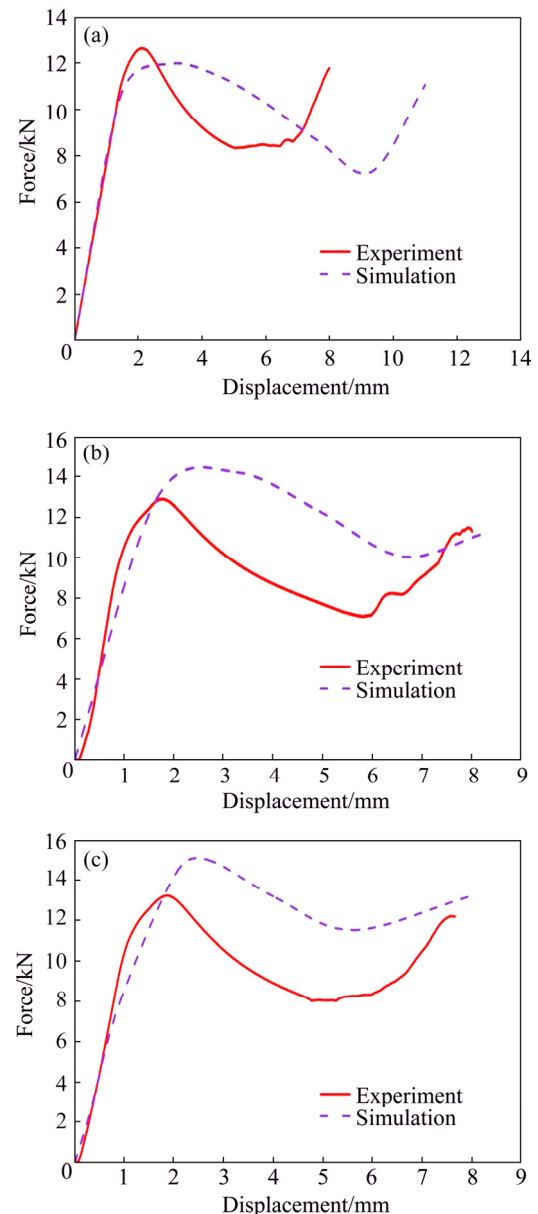


Fig. 8 Force–displacement diagrams extracted experimentally and numerically: (a) Initial thin-walled tube; (b) First PTCAP pass; (c) Second PTCAP pass

4 Conclusions

(1) Optical microscopy demonstrated that by applying the strain, grain size decreased and the microstructure of the second PTCAP pass sample contained elongated ultrafine grains.

(2) The results of mechanical properties showed that by increasing the number of PTCAP process, the tensile strength and microhardness were enhanced, continuously. The increase rate in the first PTCAP pass is much higher than those in the other passes. These variations were related to both dominant mechanisms in the PTCAP process: grain refinement and work hardening.

(3) By applying PTCAP process, deformation modes of thin-walled tubes altered from quite symmetrical and circular for annealed tubes changed to triple and double lobes diamond, for the first and the second PTCAP passes, respectively. Moreover, the deformation modes obtained from numerical simulations are completely adaptive with experimental results.

(4) After the first and second PTCAP passes, the energy absorption decreased, and the numerical investigation showed that the variation of energy absorption is consistent with experimental results. The reduction trends of the anisotropy coefficient and absorbed energy are quite similar. Also, anisotropy is the main factor associated with the rising of brittleness during PTCAP process in reducing the energy absorption capacity.

References

- [1] AFSHAR A, HASHEMI R, MADOLIAT R, RAHMATABADI D, HADIAN B. Numerical and experimental study of bursting prediction in tube hydroforming of Al 7020-T6 [J]. *Mechanics & Industry*, 2017, 18: 411–417.
- [2] ALGHAMDI A. Collapsible impact energy absorbers: An overview [J]. *Thin-walled structures*, 2001, 39: 189–213.
- [3] SADEGHI M. Design of heavy duty energy absorbers [J]. *Structural Impact and Crashworthiness*, 1984, 2: 588–604.
- [4] REID S. Metal tubes as impact energy absorbers [C]//*Metal Forming and Impact Mechanics*. Elsevier, 1985: 249–269.
- [5] MAMALIS A, MANOLOKAS D, VIEGELAHN G. The axial crushing of thin PVC tubes and frusta of square cross-section [J]. *International Journal of Impact Engineering*, 1989, 8: 241–264.
- [6] ANDREWS K, ENGLAND G, GHANI E. Classification of the axial collapse of cylindrical tubes under quasi-static loading [J]. *International Journal of Mechanical Sciences*, 1983, 25: 687–696.
- [7] GUPTA N, VENKATESH. A study of the influence of diameter and wall thickness of cylindrical tubes on their axial collapse [J]. *Thin-walled Structures*, 2006, 44: 290–300.
- [8] LI Z G, YANG H F, ZHANG Z S, SUN Y, HAN Z T, WEI J F. Crashworthiness of extruded magnesium thin-walled square tubes [J]. *Transactions of Nonferrous Metals Society of China*, 2019, 29: 1223–1232.
- [9] LINUL E, MOVAHEDI N, MARSAVINA L. The temperature effect on the axial quasi-static compressive behavior of ex-situ aluminum foam-filled tubes [J]. *Composite Structures*, 2017, 180: 709–722.
- [10] LINUL E, LELL D, MOVAHEDI N, CODREAN C, FIEDLER T. Compressive properties of zinc syntactic foams at elevated temperatures [J]. *Composites Part B: Engineering*, 2019, 167: 122–134.
- [11] ABDUL-LATIF A, BALEH R, ABOURA Z. Some improvements on the energy absorbed in axial plastic collapse of hollow cylinders [J]. *International Journal of Solids and Structures*, 2006, 43: 1543–1560.
- [12] TASDEMIRCI A. The effect of tube end constraining on the axial crushing behavior of an aluminum tube [J]. *Materials & Design*, 2008, 29: 1992–2001.
- [13] HAGHDADI N, ZAREI-HANZAKI A, ABEDI H, ABOU-RAS D, KAWASAKI M, ZHILYAEV A. Evolution of microstructure and mechanical properties in a hypoeutectic Al–Si–Mg alloy processed by accumulative back extrusion [J]. *Materials Science and Engineering A*, 2016, 651: 269–279.
- [14] CHEN X, HUANG G S, LIU S S, HAN T Z, JIANG B, TANG A T, ZHU Y T, PAN F S. Grain refinement and mechanical properties of pure aluminum processed by accumulative extrusion bonding [J]. *Transactions of Nonferrous Metals Society of China*, 2019, 29: 437–447.
- [15] FURUKAWA M, HORITA Z, NEMOTO M, LANGDAN T. Review: Processing of metals by equal-channel angular pressing [J]. *Journal of Materials Science*, 2001, 36: 2835–2843.
- [16] HASANI A, TOTH L S, BEAUSIR B. Principles of nonequal channel angular pressing [J]. *Journal of Engineering Materials and Technology*, 2010, 132: 031001–031009.
- [17] XU S B, QIN Z, LIU T, JIANG C N, REN G C. Effect of severe plastic deformation on microstructure and mechanical properties of bulk AZ31 magnesium alloy [J]. *Transactions of Nonferrous Metals Society of China*, 2012, 22: 61–67.
- [18] EBRAHIMI M, ATTARILAR S, GODE C, DJAVANROODI F. Damage prediction of 7025 aluminum alloy during equal-channel angular pressing [J]. *International Journal of Minerals, Metallurgy, and Materials*, 2014, 21: 990–998.
- [19] AZUSHIMA A, KOPP R, KORHONEN A, YANG D Y, MICARI F, LAHOTI D, GROCHE P, YANAGIMOTO J, TSUJI N, ROSOCHOWSKI A, YANAGIDA A. Severe plastic deformation (SPD) processes for metals [J]. *CIRP Annals - Manufacturing Technology*, 2008, 57: 716–735.
- [20] SAKAI G, HORITA Z, LANGDAN T. Grain refinement and superplasticity in an aluminum alloy processed by high-pressure torsion [J]. *Materials Science and Engineering A*, 2005, 393: 344–351.
- [21] ZHILYAEV A P, LANGDAN T. Using high-pressure torsion for metal processing: Fundamentals and applications [J]. *Progress in Materials Science*, 2008, 53: 893–979.
- [22] TSUJI N, SAITO Y, UTSUNOMIYA H, TANIGAWA S. Ultra-fine grained bulk steel produced by accumulative roll-bonding (ARB) process [J]. *Scripta Materialia*, 1999, 40: 795–800.

- [23] TAYYEBI M, RAHMATABADI D, ADHAMI M, HASHEMI R. Influence of ARB technique on the microstructural, mechanical and fracture properties of the multilayered Al1050/Al5052 composite reinforced by SiC particles [J]. *Journal of Materials Research and Technology*, 2019.
- [24] RAHMATABADI D, HASHEMI R, MOHAMMADI B, SHOJAEE T. Experimental evaluation of the plane stress fracture toughness for ultra-fine grained aluminum specimens prepared by accumulative roll bonding process [J]. *Materials Science and Engineering A*, 2017, 708: 301–310.
- [25] RAHMATABADI D, TAYYEBI M, HASHEMI R, FARAJI G. Microstructure and mechanical properties of Al/Cu/Mg laminated composite sheets produced by the ARB process [J]. *International Journal of Minerals, Metallurgy, and Materials*, 2018, 25: 564–572.
- [26] RAHMATABADI D, HASHEMI R. Experimental evaluation of forming limit diagram and mechanical properties of nano/ultra-fine grained aluminum strips fabricated by accumulative roll bonding [J]. *International Journal of Materials Research*, 2017, 108: 1036–1044.
- [27] RAHMATABADI D, TAYYEBI M, HASHEMI R, FARAJI G. Evaluation of microstructure and mechanical properties of multilayer Al5052–Cu composite produced by accumulative roll bonding [J]. *Powder Metall Met Ceram*, 2018, 57: 144–153.
- [28] TOTH L, ARZAGHI M, FUNDENVERGER J, BEAUSIR B, BOUAZIZ O, ARRUNFFAT-MASSION R. Severe plastic deformation of metals by high-pressure tube twisting [J]. *Scripta Materialia*, 2009, 60: 175–177.
- [29] MOHEBBI M, AKBARZADEH A. Accumulative spin-bonding (ASB) as a novel SPD process for fabrication of nanostructured tubes [J]. *Materials Science and Engineering A*, 2010, 528: 180–188.
- [30] FARAJI G, MASHHADI M, KIM H. Tubular channel angular pressing (TCAP) as a novel severe plastic deformation method for cylindrical tubes [J]. *Materials Letters*, 2011, 65: 3009–3012.
- [31] FARAJI G, BABAEI A, MASHHADI M, ABRINIA K. Parallel tubular channel angular pressing (PTCAP) as a new severe plastic deformation method for cylindrical tubes [J]. *Materials Letters*, 2012, 77: 82–85.
- [32] JAVIDIKIA M, HASHEMI R. Mechanical anisotropy in ultra-fine grained aluminium tubes processed by parallel-tubular-channel angular pressing [J]. *Materials Science and Technology*, 2017, 33: 2265–2273.
- [33] FATA A, FARAJI G, MASHHADI M, TAVAKKOLI V. Hot tensile deformation and fracture behavior of ultrafine-grained AZ31 magnesium alloy processed by severe plastic deformation [J]. *Materials Science and Engineering A*, 2016, 674: 9–17.
- [34] ABDOLVAND H, FARAJI G, GIVI M K, HASHEMI R, RIAZAT M. Evaluation of the microstructure and mechanical properties of the ultrafine grained thin-walled tubes processed by severe plastic deformation [J]. *Metals and Materials International*, 2015, 21: 1068–1073.
- [35] FARAJI G, MASHHADI M. Plastic deformation analysis in parallel tubular channel angular pressing (PTCAP) [J]. *Journal of Advanced Materials and Processing*, 2013, 1: 23–32.
- [36] GU C, LIAN J, JIANG Z, JIANG Q. Enhanced tensile ductility in an electrodeposited nanocrystalline Ni [J]. *Scripta Materialia*, 2006, 54: 579–584.
- [37] RAHMATABADI D, SHAHMIRZALOO A, FARAHANI M, TAYYEBI M, HASHEMI R. Characterizing the elastic and plastic properties of the multilayered Al/Brass composite produced by ARB using DIC [J]. *Materials Science and Engineering A*, 2019, 753: 70–78.
- [38] RAHMATABADI D, SHAHMIRZALOO A, HASHEMI R, FARAHANI M. Using digital image correlation for characterizing the elastic and plastic parameters of ultrafine-grained Al 1050 strips fabricated via accumulative roll bonding process [J]. *Materials Research Express*, 2019, 8: 086542.
- [39] FARAJI G, KIM H. Review of principles and methods of severe plastic deformation for producing ultrafine-grained tubes [J]. *Materials Science and Technology*, 2017, 33: 905–923.
- [40] KHOSHZABABN H, SANIEE F, ABEDI H R. Mechanical properties improvement of cast AZ80 Mg alloy/nanoparticles composite via thermomechanical processing [J]. *Materials Science and Engineering A*, 2014, 595: 284–290.
- [41] HOWEYZE M, ARABI H, EIVANI A, JAFARIAN H R. Strengthening of AA5052 aluminum alloy by equal channel angular pressing followed by softening at room temperature [J]. *Materials Science and Engineering A*, 2018, 720: 160–168.
- [42] BABAEI A, MASHHADI M. Tubular pure copper grain refining by tube cyclic extrusion–compression (TCEC) as a severe plastic deformation technique [J]. *Progress in Natural Science: Materials International*, 2014, 24: 623–630.
- [43] TAVAKKOLI V, AFRASIAB M, FARAJI G, MASHHADI M. Severe mechanical anisotropy of high-strength ultrafine grained Cu–Zn tubes processed by parallel tubular channel angular pressing (PTCAP) [J]. *Materials Science and Engineering A*, 2015, 625: 50–55.
- [44] AFRASIAB M, FARAJI G, TAVAKKOLI V, MASHHADI M, DEGHANI K. The effects of the multi-pass parallel tubular channel angular pressing on the microstructure and mechanical properties of the Cu–Zn Tubes [J]. *Transactions of the Indian Institute of Metals*, 2015, 68: 873–879.
- [45] RAHMATABADI D, TAYYEBI M, SHEIKHI A, HASHEMI R. Fracture toughness investigation of Al1050/Cu/MgAZ31ZB multi-layered composite produced by accumulative roll bonding process [J]. *Materials Science and Engineering A*, 2018, 734: 427–436.
- [46] RAHMATABADI D, MOHAMMADI B, HASHEMI R, SHOJAEE T. An experimental study of fracture toughness for nano/ultrafine grained Al5052/Cu multilayered composite processed by accumulative roll bonding [J]. *Journal of Manufacturing Science and Engineering*, 2018, 140: 101001–101011.
- [47] AFRASIABI M, FARAJI G, TAVAKKOLI V, MASHHADI M, AFRASIAB H. Effect of mechanical anisotropy on the energy absorption capacity in thin-walled tubes [J]. *Materials Testing*, 2017, 59: 244–248.

- [48] AFRASIABI M, FARAJI G, TAVAKKOLI V, MASHHADI M, BUSHORA A. Excellent energy absorption capacity of nanostructured Cu-Zn thin-walled tube [J]. *Materials Science and Engineering A*, 2014, 599: 141–144.
- [49] RAHMATABADI D, PAHLAVANI M, BAYATI A, HASHEMI R, MARZBANRAD J. Evaluation of fracture toughness and rupture energy absorption capacity of as-rolled LZ71 and LZ91 Mg alloy sheet [J]. *Materials Research Express*, 2019, 6: 036517.
- [50] RAHMATABADI D, HASHEMI R, TAYYEBI M, BAYATI A. Investigation of mechanical properties, formability, and anisotropy of dual phase Mg-7Li-1Zn [J]. *Materials Research Express*, 2019, 6.
- [51] PAHLAVANI M, MARZBANRAD J, RAHMATABADI D, HASHEMI R, BAYATI A. A comprehensive study on the effect of heat treatment on the fracture behaviors and structural properties of Mg-Li alloys using RSM [J]. *Materials Research Express*, 2019, 6: 076554.

PTCAP 工艺生产的 Al 5083 薄壁管 吸能能力的实验验证和数值计算

A. HOSSEINI, D. RAHMATABADI, R. HASHEMI, H. AKBARI

School of Mechanical Engineering, Iran University of Science and Technology, Tehran, Iran

摘要: 对平行管角挤压(PTCAP)工艺生产的 Al5083 薄壁管的吸能能力进行评价。研究沿周向和轴向方向的显微结构、力学性能和各向异性系数。结果表明: 能量吸收值随加工道次的增加而降低, 未处理、第一道次和第二道次处理的样品的能量吸收值分别为 167、161.4 和 160.7 J。能量吸收值的数值模拟结果与未处理的、第一和第二道次 PTCAP 处理后样品之间的误差分别约为 5%、10%和 13%。吸能能力与各向异性系数和显微结构有关。结果表明, 经过一道次和二道次 PTCAP 处理后, 晶粒得到细化, 极限抗拉强度和显微硬度均得到提高, 但一道次处理后的提高幅度更大。此外, 通过 PTCAP 处理, 变形模式发生改变, 退火后样品的变形模式非常对称且呈圆形, 而第一和第二道次变形样品的变形模式为三叶和双叶钻石形状。退火管和 PTCAP 处理管变形模式的数值模拟结果与实验结果一致。总之, 薄壁管的变形模式取决于其力学性能和 PTCAP 过程中力学性能的变化。

关键词: 吸能; Al 5083; 超细晶铝合金; 薄壁管; 大塑性变形; 各向异性系数

(Edited by Xiang-qun LI)